Temporal association between sleep spindles and ripples in the human anterior and mediodorsal thalamus

Orsolya Szalárdy[1], Péter Simor[2], Péter Przemyslaw Ujma[1], Zsófia Jordán[3], László Halász[3], Loránd Erőss[3], Dániel Fabó[3], and Róbert Bódizs[1]

[1]Semmelweis University
[2]Eötvös Loránd University
[3]National Institute of Mental Health, Neurology and Neurosurgery

December 7, 2022

Abstract

Sleep spindles are major oscillatory components of Non-Rapid Eye Movement (NREM) sleep, reflecting hyperpolarization-rebound sequences of thalamocortical neurons. Reports suggest a link between sleep spindles and several forms of high frequency oscillations which are considered as expressions of pathological off-line neural plasticity in the central nervous system. Here we investigated the relationship between thalamic sleep spindles and ripples in the anterior and mediodorsal nuclei (ANT and MD) of epilepsy patients. Whole-night LFP from the ANT and MD were co-registered with scalp EEG/polysomnography by using externalized leads in 15 epilepsy patients undergoing a Deep Brain Stimulation protocol. Slow (˜12 Hz) and fast (˜14 Hz) sleep spindles were present in the human ANT and MD and roughly, 20 % of them were associated with ripples. Ripple-associated thalamic sleep spindles were characterized by longer duration and exceeded pure spindles in terms of 100–200 Hz thalamic, but not cortical activity as indicated by time-frequency analysis. Furthermore, ripple amplitude was modulated by the phase of sleep spindles within both thalamic nuclei. No signs of pathological processes were correlated with measures of ripple and spindle association, furthermore, the density of ripple-associated sleep spindles in the ANT and MD showed a positive correlation with general intelligence. Our findings indicate the complex and multifaceted role of the human thalamus in sleep spindle-related physiological and pathological processes.

Temporal association between sleep spindles and ripples in the human anterior and mediodorsal thalamus

running title: Sleep spindles and ripples in the thalamus

Orsolya Szalárdy(1,2), Péter Simor(3,4), Péter Przemyslaw Ujma (1), Zsófia Jordán(5), László Halász(5), Loránd Erőss(5), Dániel Fabó(5), Róbert Bódizs(1)

1) Institute of Behavioural Sciences, Semmelweis University, Budapest 1089, Hungary

2) Institute of Cognitive Neuroscience and Psychology, Research Centre for Natural Sciences, Budapest 1117, Hungary

3) Institute of Psychology, ELTE, Eötvös Loránd University, Budapest 1064, Hungary

4) UR2NF, Neuropsychology and Functional Neuroimaging Research Unit at CRCN, Center for Research in Cognition and Neurosciences and UNI-ULB Neurosciences Institute, Université Libre de Bruxelles, Brussels 1050, Belgium

5) National Institute of Mental Health, Neurology and Neurosurgery, Budapest 1145, Hungary

Correspondending author: Orsolya Szalárdy, email:*szalardy.orsolya@med.semmelweis-univ.hu*

Keywords: sleep spindle; thalamic ripples; anterior thalamus; mediodorsal thalamus; general intelligence; epilepsy

Conflict of interest statement: The authors declare no competing conflict of interest.

Data Availability: Whole night thalamic LFP data are available here:*https://osf.io/q2yph/ ,https://osf.io/bz4na/,https://osf.io/temya/ ,https://osf.io/p8dqb/ ,https://osf.io/852j4/*

Author contributions: O.S. and R.B. designed research; O.S., P.S., P.P.U., Z.J., L.H., L.E., D.F., and R.B. performed research; O.S., P.S., P.P.U., Z.J., L.H., L.E., D.F., and R.B. analyzed data; O.S., P.P.U., and R.B. wrote the paper.

Acknowledgements: The work was supported by the National Research, Development and Innovation Office of Hungary Grant NKFI_FK_128100, K_128117, the ELTE Thematic Excellence Program 2020 TKP2020-IKA-05, and the Ministry of Innovation and Technology of Hungary from the National Research, Development and Innovation Fund, financed under the tkp2021-EGA-25 funding scheme.

Abstract

Sleep spindles are major oscillatory components of Non-Rapid Eye Movement (NREM) sleep, reflecting hyperpolarization-rebound sequences of thalamocortical neurons. Reports suggest a link between sleep spindles and several forms of high frequency oscillations which are considered as expressions of pathological off-line neural plasticity in the central nervous system. Here we investigated the relationship between thalamic sleep spindles and ripples in the anterior and mediodorsal nuclei (ANT and MD) of epilepsy patients. Whole-night LFP from the ANT and MD were co-registered with scalp EEG/polysomnography by using externalized leads in 15 epilepsy patients undergoing a Deep Brain Stimulation protocol. Slow (˜12 Hz) and fast (˜14 Hz) sleep spindles were present in the human ANT and **MD and roughly, 20 % of them were associated with ripples. Ripple-associated thalamic sleep spindles were characterized by longer duration and exceeded pure spindles in terms of 100–200 Hz thalamic, but not cortical activity as indicated by time-frequency analysis.** Furthermore, ripple amplitude was modulated by the phase of sleep spindles within both thalamic nuclei. No signs of pathological processes were correlated with measures of ripple and spindle association, furthermore, the density of ripple-associated sleep spindles in the ANT and MD showed a positive correlation with general intelligence. Our findings indicate the complex and multifaceted role of the human thalamus in sleep spindle-related

physiological and pathological processes.

Significance Statement: Thalamo-cortical loops are associated with sensory processing, memory formation, executive functions, many of which are tightly related with sleep state-dependent neural oscillations, such as sleep spindles. It was proposed that sleep-related epileptic transformation of normal neurological networks interfere with sleep-related synaptic homeostasis, neural plasticity, and cognitive functioning. We had a unique opportunity to investigate the association between thalamic sleep spindles and ripples, and their associations with intellectual ability within two higher-order thalamic nuclei in human subjects, the anterior thalamic and mediodorsal thalamic nuclei.

Our findings indicate the involvement of the human thalamus in sleep spindle-related physiological activity.

List of abbreviations:

AASM: American Academy of Sleep Medicine

ANT: Anterior thalamic nucleus

CT: Computed Tomography

DBS: Deep brain stimulation

EEG: Electroencephalogram

EMG: Electromyogram

FIR: Finite impulse response

IAM: Individual Adjustment Method

IEDs: Interictal epileptic discharges

IQ: General intelligence

LFP: Local field potential

M: Mean

MD: Mediodorsal thalamic nucleus

MI: Modulation index

mPFC: Medial prefrontal cortex

MRI: Magnetic Resonance Imaging

NREM: Non-rapid eye movement sleep

Ripple(NREM): Density of ripples during NREM sleep calculated as ripple number per minutes

Ripple(sp): Density of ripples during sleep spindles calculated as ripple number per minutes

SD: Standard deviation

SP(pure): pure sleep spindle

SP(ripple): ripple-associated sleep spindle

WAIS: Wechsler Adult Intelligence Scale

Introduction

Higher order brain functions rely on distributed networks involving the cortex and subcortical regions. The thalamus plays a crucial role in the proper functioning of these networks: thalamo-cortical loops are associated with sensory processing, memory formation, executive functions, many of which are tightly related with sleep state-dependent neural oscillations (Fama and Sullivan 2015; Wolff et al. 2021). The thalamus also plays an important role in the coordinated connection between the cortex and hippocampus (Latchoumane et al. 2017). The human anterior thalamic nucleus (ANT) is a higher-order thalamic nucleus which is interconnected with the hippocampus (Aggleton et al. 2010). It has reciprocal connections with the anterior cingulate cortex, retrosplenial cortex, and subiculum, and selective inactivation of the ANT leads to impaired memory formation similarly to hippocampal lesions. Furthermore, the ANT plays an important role in the propagation of epileptic seizures and therefore became an important target for deep brain stimulation (DBS) which serves as a treatment for medically refractory epilepsy (Salanova 2018). Another important higher-order nucleus in the human thalamus is the mediodorsal nucleus (MD) which is reciprocally connected with the medial prefrontal cortex (mPFC) and also receives inputs from parahippocampal regions, and therefore it is assumed to interact with the cortex and hippocampus in declarative memory formation during non-REM (NREM) sleep (Mitchell and Chakraborty 2013). Reduced MD volume was associated with decreased sleep spindle density in frontal brain regions which suggest that the MD is involved in sleep spindle generation and/or propagation (Buchmann et al. 2014).

Sleep spindles are NREM sleep state-specific oscillations characterized by waxing/waning 10–16 Hz waveforms that are generated by the reticular nucleus of the thalamus and are propagated to other brain regions by thalamo-cortical circuits (Huguenard and McCormick 2007; Steriade 2005). Animal studies confirmed that

dynamic reticular thalamic-thalamo-cortical interactions are responsible for the generation of sleep spindles (Steriade, 2005; Steriade et al., 1987), which were associated with cognitive functions such as learning and memory consolidation (Cairney et al. 2018; Saletin, Goldstein, and Walker 2011), and intellectual ability (Fogel and Smith 2011; Ujma 2018; Ujma, Bódizs, and Dresler 2020). Sleep spindles tend to co-occur with and coordinate the faster oscillations, **called hippocampal ripples (˜100–200 Hz),** providing efficient off-line plasticity windows for memory consolidation and reorganization (Girardeau and Zugaro 2011; Wilson and McNaughton 1994). Besides neural plasticity sleep spindles were associated with pathological off-line plasticity in epileptic models and human epilepsy patients (Gelinas et al. 2016). Findings regarding the strong relationship between NREM sleep oscillations, neuroplasticity and epilepsy indicate that sleep-associated interictal epileptic discharges (IEDs) harm cognitive functions, inducing a significant cognitive loss (Halász et al. 2019).

The aim of the current study was to assess the function of ANT and MD in sleep-related neural oscillations measured by the association between thalamic sleep spindles and thalamic ripples during NREM sleep. It was proposed that sleep-related epileptic transformation of normal neurological networks, involving the hippocampus, thalamus and cortex, interfere with sleep-related synaptic homeostasis, neural plasticity, and cognitive functioning (for a recent review, see Halász and Szűcs 2020). In this pathway, the role of the human ANT and MD is not clear. Although, different aspects of sleep spindle-related dynamic thalamocortical interactions were revealed (Mak-Mccully et al. 2017; Tsai et al. 2010), relationships between sleep spindles and ripples in the thalamus remained questionable. A recent report (Rektor et al. 2016) indicated the occurrence of high frequency oscillations, such as ripples in the human thalamus, however results confirming the involvement of ripples in the thalamus is remarkably sparse. Furthermore, IEDs in the human thalamus, such as in the ANT LFP records were observed and suggested the involvement of ANT in the propagation of epileptic activity and to contribute to the epileptic network (Hodaie et al. 2002; Sweeney-Reed et al. 2016). Here we investigated the association between thalamic sleep spindles and ripples within two higher-order thalamic nuclei in human subjects, the ANT and the MD. **We hypothesized that sleep spindles and ripples in these thalamic nuclei are not pathological expressions of epilepsy, but physiological oscillatory patterns. Sleep spindles, and especially fast sleep spindles measured on the scalp have a close connection with cognitive performance and intelligence (Bestmann et al. 2019; Bódizs et al. 2005; Chatburn et al. 2013; Ujma 2018). The ANT has tight anatomical and functional connections with the hippocampus, as well as different parts of the prefrontal cortex, and might act as an interface between them. In order to test the hypothesis that sleep spindles and ripples are physiological oscillations in the ANT, we assessed the association between sleep spindles and ripples with general intelligence and clinical epilepsy characteristics.**

Materials and Methods

Participants

Subjects were 15 pharmacoresistant, surgically non-treatable epilepsy patients (M_{age} = 36.9 years, range: 17–64; 7 females) participating in the ANT deep brain stimulation (DBS) protocol at the National Institute of Mental Health, Neurology and Neurosurgery, Budapest, Hungary. Clinical and demographic data are reported in Table 1. The research was approved by the ethical committee of the National Institute of Mental Health, Neurology and Neurosurgery. Patients signed informed consent for participating in the study. General intelligence (IQ) was measured prior to the surgery by Wechsler Adult Intelligence Scales, 4th edition IQ from 11 patients who underwent on neuropsychological testing in the context of their clinical routine presurgical assessment.

Experimental Design and Statistical Analysis

Procedure

A pair of quadripolar Medtronic DBS electrodes were bilaterally and stereotaxically inserted into the anterior part of the thalamus during general anaesthesia. Contact lengths of the electrode are 1.5 mm, whereas intercontact spacing is 0.5 mm. Electrode diameter is 1.27 mm. Besides frontal transventricular and ex-

traventricular trajectories, the posterior parietal extraventricular approaches were used in accordance with the decisions of the clinical-neurosurgical team. In accordance with the clinical protocol patients underwent a 48 hour, postsurgical video-EEG monitoring with externalized thalamic leads, that is thalamic LFP co-registered with scalp EEG/polygraphy. The first 48 hours were recorded without thalamic stimulation (DBS-off). One whole-night seizure-free records of the 48 hours DBS-off records were selected and analyzed in the present study.

Individual localization of thalamic contacts

Thalamic contacts were localized by using the procedure described below (see also Simor et al. 2021). In order to individually localize the thalamic contacts preoperative MRI and postoperative CT images were co-registered using tools available in the FMRIB Software Library (FSL, Oxford, FLIRT, linear registration, 6 degrees of freedom). Threshold was applied on the co-registered CT scans to achieve the desired level of density for proper identification of the lead, thus removing the surrounding brain tissue. Coordinates of the most distal point of the lead were identified and a more proximal point was selected along the line of the contacts to mathematically reconstruct the coordinates of the center point of each contact using Euclidean distance in three dimensional space. These points superimposed over the T1 MRI image provided a guideline for contact localization by examining their location to the anatomical boundaries of the ANT. Anatomical positions according to standard coordinates of the contacts were double-checked by using the mamillothalamic tract as an anatomical guide to localize the ANT. In case of convergent results of these two methods, the ANT (for 15 patients) and MD (for 10 patients) contacts were considered as subjects for further digital signal processing in the present study.

Electrophysiological data recording a preprocessing

ANT and MD LFP, and all-night sleep EEG signals were recorded by SD-LTM 64 Express EEG/polygraphic recording system. Physiological signals were recorded at 8192 Hz/channel effective sampling rate with 22 bit precision and hardware input filters set at 0.02 (high pass: 40 dB/decade) and 450 Hz (low pass: 40 dB/decade). Data was decimated by a factor of 4 by the firmware resulting in stored time series digitized at 2048 Hz/channel. LFP signals were assessed by bilateral (L – left, R – right) quadripolar electrodes applying bipolar reference scheme and focusing only on those leads which were derived from two adjacent contacts positioned in the same thalamic nucleus or alternatively from the BRIDGE area (bipolar recordings with one contact within the ANT and the second contact in adjacent tissue Deutschová et al. 2021). The number of ANT and MD derivations recorded for each patient is reported in Table 2. Scalp EEG was recorded according to the international 10-20 system (Fp1, Fp2, Fpz, F3, F4, F7, F8, C3, C4, T3, T4, T5, T6, P3, P4, O1, O2, Oz; Jasper 1958) extended with the inferior temporal chain (F9, F10, T9, T10, P9, P10) and two anterior zygomatic electrodes (ZA1, ZA2; Manzano et al. 1986), with the reference placed at the CP1 and ground placed at CP2 locations. Submental electromyograms (EMGs) were recorded by bipolarly referenced electrodes placed on the chin. For two patients (#1 and #2) the EEG electrode set up were slightly different from the above described montage. For patient #1 no Fpz, P9, P10 and EMG time series were recorded, and for patient #2 F3, F4, C3, C4, P3 and P4 electrodes were missing, although the electrode position at Pz was present in this patient. Data from missing electrodes were treated as missing values in further analyses.

Continuous EEG and LFP recordings were automatically segmented into 90 minutes chunks by the recording software. During the recording session there were no explicit light off and light on time, thus, the first and the last chunk for data analysis were selected as follows: a 90 minutes segment were required to contain at least 10 minutes of continuous sleep in the second or in the first halves, respectively for the first and last chunks. EEG data were offline re-referenced to the mathematically-linked T9 and T10 electrodes. All-night sleep records were scored for sleep-waking states and stages according to standard AASM criteria on 20 seconds basis (Berry et al. 2015) by an expert. Furthermore, artefactual segments were marked on 4 seconds basis and excluded from quantitative EEG and time series analyses.

Detection of IEDs and thalamic ripples

Data analyses were performed by MATLAB version 9.5 (R2018b, The MathWorks, Inc.,

Natick, MA; https://www.mathworks.com/products/new_products/release2018b.html) using the EEGlab toolbox 14.1.2b. For removing potential electric power-related noise, 4 Hz band-stop filter was applied centered at 50 Hz and its harmonics up to 400 Hz. For all data and frequency bands a zero-phase Hamming-windowed sinc finite impulse response (FIR) filter implemented in EEGlab (function pop_eegfiltnew contributed by A. Widmann) was used, which automatically calculates the transition bandwidth and filter order for the selected frequency bands. Ripple detection was performed on the basis of the analysis method by Gelinas et al. (2016) within the NREM stages 2 and 3 sleep. For removing potential epileptic activity (IEDs) whole-night ANT and MD LFP signals were band-pass filtered with a 25-80 Hz finite impulse response (FIR) filter. The filtered signal was then rectified and normalized. IEDs were detected as events where the filtered envelope (applying Hilbert transformation) exceeded 2 times the baseline (the mean of the filtered envelope). Those events were then eliminated where the unfiltered signal envelope was 2 times below the baseline. Where two or more IEDs occurred within 1 s, only the one with the largest amplitude was kept. For thalamic ripple detection band-pass filtering of the whole-night ANT and MD LFP signals were performed at 100–200 Hz (FIR filter). The filtered signal was then rectified and normalized. Ripples were then detected as events where the filtered envelope exceeded 5 standard deviations the baseline (the mean of the filtered envelope), and the mean envelope around the detected ripple event for a minimum of 20 ms and a maximum of 100 ms exceeded 2 standard deviation the baseline. Density of the ripples (ripple number per minutes) were calculated for the whole non-artifactual NREM sleep (in stage 2 and 3; defined as ripple(NREM) density) and for sleep spindles (i.e. the density of ripple events occurring during sleep spindle periods; defined as ripple(sp) density). Ripple(NREM) density and ripple(sp) density were compared by two-tailed Student's t-tests, separately for the ANT and MD. Statistical analyses were performed by STATISTICA 13.1 and JASP 0.15.0.0.

Sleep spindle detection and analysis

Non-artifactual NREM sleep EEG and thalamogram records were subjected to the Individual Adjustment Method (IAM) of sleep spindle analysis (Bódizs et al. 2009; Ujma et al. 2015). Frontally dominant slow and parietally dominant fast sleep spindles were defined for each patient and each EEG and thalamic channel using individual-specific frequency criteria, as well as associated individual- and derivation-specific amplitude criteria in the 9–16 Hz all-night NREM sleep. Thalamic sleep spindles contaminated with assumed IEDs (see below) were removed from further analyses, as IEDs with increased activity in the spindle frequency range may be falsely detected as spindles. The remained sleep spindles were categorized based on their association with or without ripples. If one or more ripple was detected during the spindle, that spindle was categorized as ripple-associated spindle, SP(ripple). Spindles without any association with ripples were categorized as pure sleep spindles, SP(pure). The spindle densities (number per minutes) were calculated separately for each category. Sleep spindle density data were averaged across appropriate derivations within a nucleus, separately for the ANT and MD, and for the fast and slow spindles. The duration of sleep spindles was measured as the time interval from spindle onset and offset, separately for each spindle category. Spindle duration data from all derivations corresponding to same nucleus were averaged, separately for the ANT and MD, and for the fast and slow spindles.

Overall sleep spindle density and duration were compared across nuclei performing repeated-measures ANOVA with the factors spindle type (slow vs. fast) × nucleus (ANT vs. MD), where missing values were handled as missing data. Comparison of SP(ripple/pure) density and duration were performed by repeated-measure ANOVA with the factors spindle type (slow vs. fast) × association (ripple vs. pure) × nucleus (ANT vs. MD). Post-hoc tests were conducted by Tukey's HSD.

Time-frequency wavelet analysis was performed on 4600 ms long epochs extracted in the -2300 to 2300 ms latency range around sleep spindle onsets (separately for the slow and fast SP(ripple/pure)) on all ANT and MD derivations. Furthermore, time-frequency analysis was also performed on frontal and parietal scalp records using the same time intervals as for the ANT and MD sleep spindles (scalp EEG activity around thalamic sleep spindles). Data from the F3 and F4 electrodes were analyzed for the frontal region, except for patient #15, where Fp1 was used instead of F3 due to the low signal quality. Parietal electrodes were P3 and P4, except for patient #2, where Pz was used instead of P3 and P4 as these electrodes were missing for this patient. Data were averaged across the frontal and parietal electrodes, separately. Time-frequency analysis was performed by Morlet wavelet transformation with linearly increasing cycle numbers from 4 cycles to 20 cycles for the 1–450 Hz frequency range using 0.5 Hz frequency resolution in the 1–40 Hz range, 1 Hz frequency resolution in the 41–80 Hz range and 5 Hz frequency resolution in the 81–450 Hz range. The baseline interval was set at -2000 ms to 0 ms before sleep spindle onset. Time-frequency power spectra were averaged across all derivations within the same nucleus, separately for the fast and slow SP(ripple/pure). Statistical comparison of SP(ripple) vs. SP(pure) was performed by nonparametric randomization test separately for the slow and fast spindles and for the ANT, MD and scalp (frontal and parietal), applying the Monte-Carlo estimate of significance probabilities (1000 permutations), using the Fieldtrip toolbox (Oostenveld et al. 2011), applying FDR correction.

For assessing phase-amplitude coupling between sleep spindle phases and ripple amplitudes in the thalamus, the modulation index (MI) was calculated based on the method by Tort et al. (2010), separately for each thalamic derivation. First, 4600 ms long epochs were extracted around individual sleep spindles with co-occurring ripples (SP(ripple)), in the -2300 to 2300 ms latency range where 0 ms corresponds to the onset of sleep spindles. For all detected SP(ripple) data were band-pass filtered in the frequency bands of interest, 80–200 Hz for extracting the ripple amplitude and individual slow and fast spindle bands, detected by the IAM of sleep spindle analysis (see above) for extracting instantaneous phase of sleep spindles (FIR filter). Bandpass-filtered data were than Hilbert transformed using the 0–2000 ms time range for avoiding edge effects. MI were then calculated for each electrode using 18 phase bins from $-\pi$ to $+\pi$, pooling all phase and amplitude values extracted from the epoched data. The observed MI were then subjected to permutation testing in order to quantify the difference between the observed MI and the distribution of shuffled coupling values. Shuffled MI distribution were calculated by measuring the MI between the original phase time series and permuted amplitude time series where amplitude data points were randomly shuffled, using 1000 iterations for each electrode. The observed MI values were then z-standardized to the shuffled phase-amplitude coupling distribution, where normalized z-values directly reflect p-values, MI(z) equal to 1.645 corresponds to the 5% p-value. Thus, MI(z) values larger than 1.645 reflects a significant spindle-ripple coupling in the thalamus.

We aimed to estimate the time dynamics of spindle co-occurrence between thalamic and cortical channels. **Spindle co-occurrence was defined in the following way: when the initiation of a sleep spindle was detected on any channel (cortical or thalamic), all subsequent spindles initiating on any other channel before the end of the original spindle were considered to co-occur, comprising a single spindle event involving multiple channels with a time lag on each channel, defined as the time difference of spindle initiation relative to the first spindle. For thalamocortical co-occurrence analysis, we selected all instances when sleep spindles co-occurred on both 1) a selected scalp channel (F3 or F4 for frontal spindles, P3 or P4 for parietal spindles, for patient #2 Fp2-Fpz and Pz-Oz instead) and 2) on a channel localized in a specific thalamic nucleus (ANT or MD). That is, the analysis included spindles which could originate elsewhere, but were later detected on both specific scalp channels and in the thalamus. We defined thalamocortical spindle lags as the time lag (relative to the first spindle) of the scalp channel minus the time lag of the thalamic channel. We modeled spindle lags with a linear mixed model implemented in the MATLAB 2017a fitlme() function using lag as the dependent variable, spindle type, thalamic nucleus and scalp channel as fixed effects with random intercepts by patient (Ujma et al. 2022).**

For assessing the potential correlates and functions of thalamic ripples and spindles Pearson correlations

coefficient were calculated between sleep spindle density (scalp-detected parietal fast sleep spindle density, overall thalamic spindle density, thalamic SP(ripple) and SP(pure) density), clinical epilepsy characteristics (years since epilepsy onset and seizures/month (before DBS)), and general intelligence (**Table 3 shows the WAIS IQ scores**); separately for the ANT and MD, and for the slow and fast spindles. Relationships between scalp-detected, parietal fast sleep spindle density were measured based on the average recording locations P3 and P4, except Patient #2, where Pz was used.

Results

Ripple density during sleep spindles and overall NREM sleep

Ripple(NREM) and ripple(sp) density were not significantly different from each other (Figure 1) in the ANT ($t_{14} = 1.427$, $p = 0.176$) but a significant difference was found in the MD ($t_9 = 2.293$,$p = 0.048$), where the ripple(sp) density was larger than the ripple(NREM) density, indicating the more frequent coupling of ripples to sleep spindles compared to spindle-free NREM periods.

Overall sleep spindle density and duration in the ANT and MD

For the overall sleep spindle density (Figure 2), main effect of spindle type and nucleus was not significant (nucleus:$F_{1,9} = 3.432$, $p = 0.097$ spindle type:$F_{1,9} = 3.490$, $p = 0.095$), but there was a significant interaction between these factors ($F_{1,9} = 6.203$, $p = 0.034$). Post-hoc test revealed that the interaction was caused by the significantly lower fast spindle density in the MD compared to the ANT (p = 0.039). Main effect of spindle type was significant for the duration of sleep spindles ($F_{1,9} = 5.756$, $p = 0.040$) due to the longer slow sleep spindles compared to fast sleep spindles. Main effect of nucleus was not significant ($F_{1,9} = 0.126$,$p = 0.730$) and no interaction occurred between these factors ($F_{1,9} = 2.621$, $p = 0.140$) on the duration of sleep spindles.

Sleep spindle density and duration (SP(pure/ripple) in the ANT and MD associated with and without ripples

Φιγυρε 3. σηοως εξαμπλες φορ φαστ σλεεπ σπινδλες φρομ τηε σαμε πατιεντ ανδ νυ-ςλευς, ασσοςιατεδ ωιτη ανδ ωιτηουτ ριππλες. Σιγνιφιςαντ μαιν εφφεςτ οφ ασσοςιατιον ωας φουνδ φορ τηε σπινδλε δενσιτψ ($\Phi_{1,9} = 53.180$, $\pi < 0.001$,$\eta\pi^2 = 0.855$), δυε το τηε ηιγηερ ΣΠ(πυρε) δενσιτψ ςομπαρεδ το τηε ΣΠ(ριππλε) δενσιτψ. Τηε μαιν εφφε-ςτ οφ σπινδλε τψπε ανδ νυςλευς ωας νοτ σιγνιφιςαντ (σπινδλε τψπε:$\Phi_{1,9} = 3.489$, $\pi = 0.095$,$\eta\pi^2 = 0.279$· νυςλευς:$\Phi_{1,9} = 3.432$, $\pi = 0.097$,$\eta\pi^2 = 0.276$), βυτ σιγνιφιςαντ ιντεραςτιον οςςυρρεδ βετωεεν τηεσε φαςτορς ($\Phi_{1,9} = 6.202$,$\pi = 0.034$, $\eta\pi^2 = 0.408$). Ποστ-ηος τεστ ρεεαλεδ τηατ τηε ιντεραςτιον ωας δυε το τηε σιγνιφιςαντλψ λοωερ φαστ σλεεπ σπινδλε δενσιτψ ιν τηε ΜΔ ςομπαρεδ το τηε ΑΝΤ ($\pi = 0.027$). Τηε δυρατιον οφ σλεεπ σπινδλες ωας αφφεςτεδ βψ τηε ριππλε-ασσοςιατιον, ας ινδιςατεδ βψ τηε σιγνιφι-ςαντ μαιν εφφεςτ οφ ασσοςιατιον ($\Phi_{1,9} = 54.661$, $\pi < 0.001$,$\eta\pi^2 = 0.858$), ον αεραγε, ριππλε-ασσοςιατεδ σπινδλες ωερε 232 μς λονγερ τηαν πυρε σπινδλες (Φιγυρε 4). Τηε μαιν εφφεςτ οφ σπινδλε τψπε ωας αλσο σιγνιφιςαντ, ας λονγερ σλοω σπινδλες ωερε δετεςτεδ ςομπαρεδ το τηε φαστ σπινδλες ($\Phi_{1,9}$= 5.577, $\pi = 0.0425$, $\eta\pi^2 = 0.383$). Τηε μαιν εφφεςτ οφ νυςλευς ωας νοτ σιγνιφιςαντ ($\Phi_{1,9}$= 0.404, $\pi = 0.541$, $\eta\pi^2 = 0.043$), ανδ νο ιντεραςτιον οςςυρρεδ βετωεεν τηε φαςτορς ($\pi > 0.137$, ατ λεαστ).

Power spectral density in the time-frequency domain of pure and ripple-associated spindles

SP(pure) and SP(ripple) were characterized by comparable spindle frequency power (11–16 Hz) in both thalamic nuclei (ANT and MD) between 0-500 ms from the onset of sleep spindles, while increased power was observed between 5-15 Hz later, beginning from 500-1200 ms for the slow sleep spindles in the ANT (Figure 5). Similar results were found for the ANT fast spindles, however, the low-frequency difference was less pronounced (see Supplementary material). The 100–200 Hz power of ANT slow and fast SP(ripple) exceeded the corresponding power values

of SP(pure) up to around 1000 ms. In the MD, the same contrast resulted in significant differences for fast spindles, but not for slow spindles. Thalamic SP(pure) and SP(ripple) did not differ in terms of concomitant scalp EEG time-frequency power (see Figure 5. for ANT slow sleep spindles, the ANT fast and MD spindles are presented in the Supplementary material).

Spindle-ripple coupling in the thalamus

For all electrode position, the permutation test revealed that the observed MI were significantly larger than the permuted MI (all p's < 0.001, except a single MI value for the slow sleep spindles in one ANT derivation for patient #2, where $p = 0.019$), both in the ANT and MD, separately for the slow and fast sleep spindles (MI_Z ANT fast spindle: 22.56, $p < 0.001$, SD: 19.00; MI_Z ANT slow spindle: 22.01,$p < 0.001$, SD: 15.93; MI_Z MD fast spindle: 92.07, $p < 0.001$, SD: 224.09; MI_Z MD slow spindle: 89.54, $p < 0.001$,SD: 201.83). Figure 5 shows a representative example for spindle phase and ripple coupling in the ANT.

Spindle dynamics in the thalamus and the cortex

Τηε διστριβυτιον οφ τηαλαμοςορτιςαλ λαγς (βροκεν δοων βψ ριππλε ςο-οςςυρρενςε) ις σηοων ον Φιγυρε 7. Ιν σηορτ, τηαλαμοςορτιςαλ λαγς ωερε γενεραλλψ ειτηερ νεγατιε ορ νοτ σιγνιφιςαντλψ διφφερεντ φρομ ζερο, ινδιςατινγ τηατ ειτηερ σλεεπ σπινδλες πρεφερεντιαλλψ οςςυρρεδ ον τηε σςαλπ φιρστ ορ οςςυρρεδ σιμυλτανεουσλψ ον σςαλπ ανδ τηαλαμις ςηαννελς. Ἐρψ λιττλε αριανςε ιν σπινδλε λαγ ωας αςςουντεδ φορ βψ τηις μοδελ ($P2 = 0.014$), συγγεστινγ τηατ λαγ μαινλψ δεπενδς ον εξτρανεους φαςτορς. Στιλλ, φαστ σπινδλες ($\beta = 0.015$), σπινδλες ιν τηε ΜΔ νυςλευς ($\beta = 0.017$) ανδ σπινδλες οςςυρρινγ ον Φ4 ($\beta = 0.010$) ωερε ασσοςιατεδ ωιτη μορε ποσιτιε λαγς, ωηιλε σπινδλες οςςυρρινγ ον Π3 ($\beta =$ -0.007) ανδ σπινδλες ωιτη ριππλες ($\beta =$ -0.017) ωερε ασσοςιατεδ ωιτη μορε νεγατιε λαγς. Τηατ ις, ιν ςασε οφ φαστ σπινδλες, ιν τηε ΜΔ ανδ ον Φ4, τηερε ωας α διμινισηεδ τενδενςψ φορ σςαλπ σπινδλες το οςςυρ φιρστ, βυτ τηις τενδενςψ ινςρεασεδ ον Π3 ανδ εσπεςιαλλψ ωηεν ριππλε αςτιιτψ ωας πρεσεντ ιν τηε τηαλαμυς. Αλλ εφφεςτ σιζες αρε υνστανδαρδιζεδ ανδ γιεν ιν σεςονδς. Αλλ $\pi<0.001$, εξςεπτ φορ τηε εφφεςτ ασσοςιατεδ ωιτη Π3 ($\pi = 0.010$).

The relation between thalamic spindles, clinical epilepsy characteristics, and general intelligence

Statistical analysis revealed a significant negative correlation between slow SP(pure) density in the MD and the years since epilepsy onset (Figure 7; $r =$ -0.653, $N = 10$, $p = 0.040$), whereas the fast SP(pure) density in the same nucleus correlated positively with the seizure prevalence ($r = 0.633$, $N = 10$,$p = 0.050$). No significant correlation occurred between the ANT spindle density (SP(pure) and SP(ripple)) and years since epilepsy onset ($p > 0.061$), and with seizure prevalence ($p > 0.384$).

The overall density of sleep spindles did not show significant correlation with IQ, neither in the ANT ($r = 0.139$, $p = 0.682$ for slow and $r = 0.029$, $p = 0.932$ for fast sleep spindles, $N = 11$), nor in the MD ($r = 0.311$, $p = 0.497$ for slow and $r =$ -0.523, $p = 0.229$ for fast sleep spindles, $N = 7$). Furthermore, the association of fast spindle density measured on the scalp with IQ did not reach the specified alpha level ($r = 0.399$, $p = 0.225$, $N = 11$). However, when thalamic sleep spindles were separated according to their associations with and without ripples, positive correlations were observed between IQ and fast SP(ripple) density in the ANT ($r = 0.778$, $N = 11$,$p = 0.0055$) and slow SP(ripple) density in the MD ($r = 0.808$, $N = 11$, $p < 0.028$).

Discussion

We investigated the occurrence of sleep spindles and ripples in the human anterior and mediodorsal thalamus and those associations with epilepsy characteristics and general intelligence. **Sleep spindles were detected**

both in the ANT and MD. The occurrence of sleep spindles in the human ANT were confirmed in previous studies (Tsai et al. 2010). We demonstrated that spindles are also present in the human MD. The duration of slow and fast spindles was similar in the two thalamic nuclei, however the overall density of fast sleep spindles was lower in the MD compared to the ANT. In the majority of cases where thalamic-scalp sleep spindle co-occurrences were detected, ANT and MD sleep spindles slightly lagged behind cortical ones, which coheres with available reports (Tsai et al. 2010) and suggests the prevailing role of corticofugal fibers in the herein studied phenomena. In a recent study, Bastuji et al. (2020) recorded sleep spindles from different parts of the posterior thalamus. These results indicate that anterior, mediodorsal and posterior thalamic nuclei are involved in the proper functioning of the NREM sleep-related thalamo-cortical network generating mid-frequency oscillations in the burst-firing mode.

In addition of detecting thalamic sleep spindles in human subjects, we revealed their association with thalamic ripples. SP(ripple) made up around 20% of overall ANT and MD sleep spindles, respectively. These spindles were of longer duration and characterized by different time-frequency activity profiles than sleep spindles in the absence of ripples: SP(ripple) were associated with an excess of thalamic ripple and lower (5-15 Hz) frequency activity compared to SP(pure). This 5-15 Hz activity occurred later, roughly 500 ms after sleep spindle onset, which is assumed to reflect the elongation of ripple-associated sleep spindles. The increased ripple-band activity was the basis of ripples-associated sleep spindle definition; however, no signs of power difference were observed in the same time window at scalp derivations.

The coordinated interactions between hippocampal ripples and cortical sleep spindles plays crucial role in memory formation (Latchoumane et al. 2017; Siapas and Wilson 1998; Staresina et al. 2015). It was proposed that NREM sleep-based memory formation depends on the hierarchical nesting of slow waves, sleep spindles and hippocampal ripples, as these oscillations are instrumental in transferring information from the hippocampus to the neocortex (Diekelmann and Born 2010; Staresina et al. 2015). In the past few years, accumulating evidence were found for the existence of ripples outside of the hippocampus (for a review, see McKenzie, Nitzan, and English 2020). Ripples were detected in several cortical areas such as somatosensory and motor cortices (Averkin et al. 2016), olfactory cortices (Manabe et al. 2011), parahippocampal regions (Axmacher, Elger, and Fell 2008) and higher order associational cortices as well (Khodagholy, Gelinas, and Buzsáki 2017). These cortical ripples were frequently coupled with slower oscillations including sleep spindles. In the prefrontal cortex, mesio-temporal and neocortical structures, ripples were detected both before sleep spindles and locked to the spindle troughs (Bruder et al. 2021; Peyrache, Battaglia, and Destexhe 2011). Similar results were observed confirming that cortical ripples were embedded into spindle troughs during natural sleep (Averkin et al. 2016). **Although it is not entirely clear, whether ripples in the thalamus are connected with pathological processes related to epilepsy. A close relationship between epilepsy and high-frequency oscillations (80–600 Hz, HFOs) occurrence is repeatedly found in animal and human studies (for a review, see Jiruska et al. 2017). In a recent study, Rektor et al. (2016) found HFOs during wakefulness in the human ANT up to 240 Hz frequency, and 500 Hz frequency in one case, which was the first report of HFOs in the human thalamus. Deutschová et al (2021) reported a relationship between prestimulation HFO power and ANT-BDS treatment reponse, with reduced awake resting 65–500 Hz activity forecasting better outcome. In the current study, ripples (100–200 Hz) were revealed in both ANT and MD nuclei during NREM sleep. Ripple events were in part coupled with sleep spindles, but also detected outside spindles during NREM sleep. We found a strong phase-amplitude coupling measured by the modulation index between sleep spindle phase and ripple amplitude. However, thalamic 100–200 Hz ripples emerging during sleep spindles were not associated with pathological processes, rather, SP(ripple) were shown to indicate preserved cognitive ability. Here we found a positive correlation between the density of SP(ripple) in the ANT and general intelligence (overall cognitive functions) of our patients. This latter result indicates that 100–200 Hz ripples detected in the human ANT during NREM sleep spindles may contribute to**

the physiological expression of thalamocortical oscillations. Furthermore, these results suggest that thalamic ripples could indicate physiological forms of neural activity.

The temporal dynamics of sleep spindles in the thalamus and the scalp show that cortical spindle preceded thalamic spindles, especially those associated with ripples. Sleep spindles are generated by the reticular thalamic nucleus and propagate to the cortex through thalamo-cortical network (Steriade 2005; Steriade et al. 1987). The temporal advantage of the scalp sleep spindles suggest that ANT and MD sleep spindles are propagated through cortico-thalamic networks, and not directly through thalamo-thalamic projections. It was suggested that cortico-thalamic feedback projections from the cortical sites to the reticular thalamus is responsible for the large-scale synchronization of sleep spindles (Destexhe, Contreras, and Steriade 1998). The ANT has a bidirectional connection with the anterior cingulate cortex, retrosplenial cortex, and subiculum, whereas the MD is interconnected with the medial-prefrontal cortex (Aggleton et al. 2010; Mitchell and Chakraborty 2013; Pergola et al. 2018). The recent results suggest that sleep spindles propagate through these cortical sites to the ANT and MD. Thus, the thalamus seems to play an important interface between the propagation of these neural oscillations in the hippocampal-prefrontal network.

Former studies suggested that the human ANT contribute to the epileptic network, and the ANT became an important target for DBS in epilepsy treatment (Hodaie et al. 2002; Salanova 2018; Sweeney-Reed et al. 2016). Furthermore, interictal discharges were also detected in the MD (Sweeney-Reed et al. 2016). Although, there is no direct anatomical connection between the ANT and MD, this report indicates that the MD might be involved in the epileptic circuitry as well. Our current results further support this assumption. Besides interictal discharges, the presence of different sleep spindle (slow vs fast) could be also indicative for specific network dysfunctions. The density of slow SP(pure) in the MD showed a negative correlation with the year since epilepsy onset. In contrast to slow spindles, fast SP(pure) density showed a positive correlation with seizure prevalence. These results suggest that the ANT and MD are involved in different epileptogenic circuitries. The occurrence of fast sleep spindles may indicate the altered functioning of the MD due to network-based changes through epilepsy propagation, whereas the occurrence of fast spindles seems physiological in the ANT**. This was also indicated by the lower overall fast spindle density in the MD.** Sleep spindles in the mediodorsal thalamus were also indicative in schizophrenia patients, where a negative association were found between the volume of the MD and scalp-recorded sleep spindle density (Ferrarelli and Tononi 2017). To our best knowledge, this is the first report where sleep spindles were separated to fast and slow spindles, showing that the appearance of fast sleep spindles may indicate pathological mechanisms in the mediodorsal thalamic functions.

The current results support the involvement of the human thalamus in sleep spindle-related neural activity. Sleep spindles were found in the ANT and in the MD and ripples coupled with sleep spindles resulted in distinguishable spectro-temporal differences in the thalamus but not at the scalp. The major finding is that ripples are also present in the thalamus, which seems to contribute to intellectual ability through a tight interaction between spindles and ripples. Limitations of the study are the lack of direct testing of offline memory processes during sleep. Also, the sample size is too low to reveal the specific IQ subscores which are influenced by the coordinated activity of sleep spindles and ripples in the thalamus. Co-registration from the hippocampus, thalamus and scalp will present an opportunity to reveal the hippocampal-thalamo-cortical pathway in further research, providing target circuits for neuromodulation and therapeutics. Furthermore, our participants suffered from medically refractory epilepsy being subjects of poly-antiseizure medication treatment. This type of treatment was shown to reduce sleep slow wave (0.1-2 Hz) EEG amplitude, increase sleep spindle frequency (11-16 Hz) power, and decrease slow wave-sleep spindle cross-frequency coupling in epilepsy patients (Roebber et al. 2022). As our present investigation focuses on sleep spindle-related activity of epilepsy patients we cannot entirely exclude the possibility that our reported findings are indeed partially influenced by antiseizure medications. Further investigations focusing on the thalamic recordings of patients groups with different medication are needed in order to provide unequivocal evidence for the claims we made in our paper.

References

Aggleton, J. P., S. M. O'Mara, S. D. Vann, N. F. Wright, M. Tsanov, and J. T. Erichsen. 2010. "Hippocampal-Anterior Thalamic Pathways for Memory: Uncovering a Network of Direct and Indirect Actions." *European Journal of Neuroscience* 31(12):2292–2307.

Averkin, R. G., V. Szemenyei, S. Bordé, and G. Tamás. 2016. "Identified Cellular Correlates of Neocortical Ripple and High-Gamma Oscillations during Spindles of Natural Sleep." *Neuron* 92(4):916–28.

Axmacher, N., C. E. Elger, and J. Fell. 2008. "Ripples in the Medial Temporal Lobe Are Relevant for Human Memory Consolidation." *Brain : A Journal of Neurology* 131(Pt 7):1806–17.

Bastuji, H., P. Lamouroux, M. Villalba, M. Magnin, and L. Garcia-Larrea. 2020. "Local Sleep Spindles in the Human Thalamus." *The Journal of Physiology* 598(11):2109–24.

Berry, R. B., R. Brooks, C. E. Gamaldo, S. M. Harding, R. M. Lloyd, C. L. Marcus, and B. V. Vaughn. 2015. *AASM | Scoring Manual Version 2.2 The AASM Manual for the Scoring of Sleep and Associated Events RULES, TERMINOLOGY AND TECHNICAL SPECIFICATIONS VERSION 2.2* .

Bodizs, R., J. Kormendi, P. Rigo, and A. S. Lazar. 2009. "The Individual Adjustment Method of Sleep Spindle Analysis: Methodological Improvements and Roots in the Fingerprint Paradigm." *Journal of Neuroscience Methods* 178(1):205–13.

Bruder, J. C., C. Schmelzeisen, D. Lachner-Piza, P. Reinacher, A. Schulze-Bonhage, and J. Jacobs. 2021. "Physiological Ripples Associated With Sleep Spindles Can Be Identified in Patients With Refractory Epilepsy Beyond Mesio-Temporal Structures." *Frontiers in Neurology* 0:48.

Buchmann, A., D. Dentico, M. J. Peterson, B. A. Riedner, S. Sarasso, M. Massimini, G. Tononi, and F. Ferrarelli. 2014. "Reduced Mediodorsal Thalamic Volume and Prefrontal Cortical Spindle Activity in Schizophrenia." *NeuroImage* 102(P2):540–47.

Cairney, S. A., A. V. Guttesen, N. E. Marj, and B. P. Staresina. 2018. "Memory Consolidation Is Linked to Spindle-Mediated Information Processing during Sleep." *Current Biology* 28(6):948.

Destexhe, A., D. Contreras, and M. Steriade. 1998. "Mechanisms Underlying the Synchronizing Action of Corticothalamic Feedback through Inhibition of Thalamic Relay Cells." *Journal of Neurophysiology*79(2):999–1016.

Deutschova, B., P. Klimeš, Z. Jordan, P. Jurák, L. Erőss, M. Lamoš, J. Halámek, P. Daniel, I. Rektor, and D. Fabo. 2021. "Thalamic Oscillatory Activity May Predict Response to Deep Brain Stimulation of the Anterior Nuclei of the Thalamus." *Epilepsia* 62(5):e70–75.

Diekelmann, S., and J. Born. 2010. "The Memory Function of Sleep." *Nature Reviews Neuroscience* 11(2):114–26.

Fama, R., and E. V. Sullivan. 2015. "Thalamic Structures and Associated Cognitive Functions: Relations with Age and Aging." *Neuroscience and Biobehavioral Reviews* 54:29.

Ferrarelli, F., and G. Tononi. 2017. "Reduced Sleep Spindle Activity Point to a TRN-MD Thalamus-PFC Circuit Dysfunction in Schizophrenia." *Schizophrenia Research* 180:36–43.

Fogel, S. M., and C. T. Smith. 2011. "The Function of the Sleep Spindle: A Physiological Index of Intelligence and a Mechanism for Sleep-Dependent Memory Consolidation." *Neuroscience and Biobehavioral Reviews* 35(5):1154–65.

Gelinas, J. N., D. Khodagholy, T. Thesen, O. Devinsky, and G. Buzsáki. 2016. "Interictal Epileptiform Discharges Induce Hippocampal-Cortical Coupling in Temporal Lobe Epilepsy." *Nature Medicine*22(6):641–48.

Girardeau, G., and M. Zugaro. 2011. "Hippocampal Ripples and Memory Consolidation." *Current Opinion in Neurobiology* 21(3):452–59.

Halász, P., R. Bódizs, P. P. Ujma, D. Fabó, and A. Szűcs. 2019. "Strong Relationship between NREM Sleep, Epilepsy and Plastic Functions — A Conceptual Review on the Neurophysiology Background." *Epilepsy Research* 150:95–105.

Halász, P., and A. Szűcs. 2020. "Sleep and Epilepsy Link by Plasticity." *Frontiers in Neurology* 11:911.

Hodaie, M., R. A. Wennberg, J. O. Dostrovsky, and A. M. Lozano. 2002. "Chronic Anterior Thalamus Stimulation for Intractable Epilepsy." *Epilepsia* 43(6):603–8.

Huguenard, J. R., and D. A. McCormick. 2007. "Thalamic Synchrony and Dynamic Regulation of Global Forebrain Oscillations." *Trends in Neurosciences* 30(7):350–56.

Jasper, H. H. 1958. "The Ten-Twenty Electrode System of the International Federation." *Electroencephalography and Clinical Neurophysiology* 10:371–75.

Jiruska, P., C. Alvarado-Rojas, C. A. Schevon, R. Staba, W. Stacey, F. Wendling, and M. Avoli. 2017. "Update on the Mechanisms and Roles of High-Frequency Oscillations in Seizures and Epileptic Disorders." *Epilepsia* 58(8):1330–39.

Khodagholy, D., J. N. Gelinas, and G. Buzsáki. 2017. "Learning-Enhanced Coupling between Ripple Oscillations in Association Cortices and Hippocampus." *Science (New York, N.Y.)* 358(6361):369–72.

Latchoumane, C. F. V., H. V. V. Ngo, J. Born, and H. S. Shin. 2017. "Thalamic Spindles Promote Memory Formation during Sleep through Triple Phase-Locking of Cortical, Thalamic, and Hippocampal Rhythms." *Neuron* 95(2):424-435.e6.

Mak-Mccully, R. A., M. Rolland, A. Sargsyan, C. Gonzalez, M. Magnin, P. Chauvel, M. Rey, H. Bastuji, and E. Halgren. 2017. "Coordination of Cortical and Thalamic Activity during Non-REM Sleep in Humans." *Nature Communications* 8(1):1–11.

Manabe, H., I. Kusumoto-Yoshida, M. Ota, and K. Mori. 2011. "Olfactory Cortex Generates Synchronized Top-down Inputs to the Olfactory Bulb during Slow-Wave Sleep." *The Journal of Neuroscience : The Official Journal of the Society for Neuroscience* 31(22):8123–33.

Manzano, G. M., P. C. Ragazzo, S. M. Tavares, and R. Marino Jr. 1986. "Anterior Zygomatic Electrodes: A Special Electrode for the Study of Temporal Lobe Epilepsy." *Stereotactic and Functional Neurosurgery* 49(4):213–17.

McKenzie, S., N. Nitzan, and D. F. English. 2020. "Mechanisms of Neural Organization and Rhythmogenesis during Hippocampal and Cortical Ripples." *Philosophical Transactions of the Royal Society B*375(1799).

Mitchell, A. S., and S. Chakraborty. 2013. "What Does the Mediodorsal Thalamus Do?" *Frontiers in Systems Neuroscience* (JUL).

Oostenveld, R., P. Fries, E. Maris, and J. M. Schoffelen. 2011. "FieldTrip: Open Source Software for Advanced Analysis of MEG, EEG, and Invasive Electrophysiological Data." *Computational Intelligence and Neuroscience* 2011.

Pergola, G., L. Danet, A. L. Pitel, G. A. Carlesimo, S. Segobin, J. Pariente, B. Suchan, A. S. Mitchell, and E. J. Barbeau. 2018. "The Regulatory Role of the Human Mediodorsal Thalamus." *Trends in Cognitive Sciences* 22(11):1011–25.

Peyrache, A., F. P. Battaglia, and A. Destexhe. 2011. "Inhibition Recruitment in Prefrontal Cortex during Sleep Spindles and Gating of Hippocampal Inputs." *Proceedings of the National Academy of Sciences of the United States of America* 108(41):17207–12.

Rektor, I., I. Doležalová, J. Chrastina, P. Jurák, J. Halámek, M. Baláž, and M. Brázdil. 2016. "High-Frequency Oscillations in the Human Anterior Nucleus of the Thalamus." *Brain Stimulation*9(4):629–31.

Roebber, J. K., P. A. Lewis, V. Crunelli, M. Navarrete, and K. Hamandi. 2022. "Effects of Anti-Seizure Medication on Sleep Spindles and Slow Waves in Drug-Resistant Epilepsy." *Brain Sciences* 12(10):1288.

Salanova, V. 2018. "Deep Brain Stimulation for Epilepsy." *Epilepsy and Behavior* 88:21–24.

Saletin, J. M., A. N. Goldstein, and M. P. Walker. 2011. "The Role of Sleep in Directed Forgetting and Remembering of Human Memories." *Cerebral Cortex (New York, NY)* 21(11):2534.

Siapas, A. G., and M. A. Wilson. 1998. "Coordinated Interactions between Hippocampal Ripples and Cortical Spindles during Slow-Wave Sleep." *Neuron* 21(5):1123–28.

Simor, P., O. Szalárdy, F. Gombos, P. P. Ujma, Z. Jordán, L. Halász, L. Erőss, D. Fabó, and R. Bódizs. 2021. "REM Sleep Microstates in the Human Anterior Thalamus." *The Journal of Neuroscience*JN-RM-1899-20.

Staresina, B. P., T. O. Bergmann, M. Bonnefond, R. Van Der Meij, O. Jensen, L. Deuker, C. E. Elger, N. Axmacher, and J. Fell. 2015. "Hierarchical Nesting of Slow Oscillations, Spindles and Ripples in the Human Hippocampus during Sleep." *Nature Neuroscience*18(11):1679–86.

Steriade, M. 2005. "Sleep, Epilepsy and Thalamic Reticular Inhibitory Neurons." *Trends in Neurosciences* 28(6 SPEC. ISS.):317–24.

Steriade, M., L. Domich, G. Oakson, and M. Deschenes. 1987. "The Deafferented Reticular Thalamic Nucleas Generates Spindle Rhythmicity." *Journal of Neurophysiology* 57(1):260–73.

Sweeney-Reed, C. M., H. Lee, S. Rampp, T. Zaehle, L. Buentjen, Juergen Voges, Martin Holtkamp, Hermann Hinrichs, Hans Jochen Heinze, and Friedhelm C. Schmitt. 2016. "Thalamic Interictal Epileptiform Discharges in Deep Brain Stimulated Epilepsy Patients." *Journal of Neurology* 263(10):2120–26.

Tort, A. B. L., R. Komorowski, H. Eichenbaum, and N. Kopell. 2010. "Measuring Phase-Amplitude Coupling between Neuronal Oscillations of Different Frequencies." *Journal of Neurophysiology*104(2):1195–1210.

Tsai, Y. T., H. L. Chan, S. T. Lee, P. H. Tu, B. L. Chang, and T. Wu. 2010. "Significant Thalamocortical Coherence of Sleep Spindle, Theta, Delta, and Slow Oscillations in NREM Sleep: Recordings from the Human Thalamus." *Neuroscience Letters* 485(3):173–77.

Ujma, P. P. 2018. "Sleep Spindles and General Cognitive Ability – A Meta-Analysis." *Sleep Spindles & Cortical Up States*1(aop):1–17.

Ujma, P. P., R. Bódizs, and M. Dresler. 2020. "Sleep and Intelligence: Critical Review and Future Directions." *Current Opinion in Behavioral Sciences* 33:109–17.

Ujma, P. P., F. Gombos, L. Genzel, B. N. Konrad, P. Simor, A. Steiger, M. Dresler, and R. Bódizs. 2015. "A Comparison of Two Sleep Spindle Detection Methods Based on All Night Averages: Individually Adjusted vs. Fixed Frequencies." *Frontiers in Human Neuroscience* 9(FEB):52.

Ujma, P. P., O. Szalárdy, D. Fabó, L. Erőss, and R. Bódizs. 2022. "Thalamic Activity during Scalp Slow Waves in Humans." *NeuroImage* 257:119325.

Wilson, M. A., and B. L. McNaughton. 1994. "Reactivation of Hippocampal Ensemble Memories During Sleep." *Science* 265(5172):676–79.

Wolff, M., S. Morceau, R. Folkard, J. Martin-Cortecero, and A. Groh. 2021. "A Thalamic Bridge from Sensory Perception to Cognition." *Neuroscience & Biobehavioral Reviews* 120:222–35.

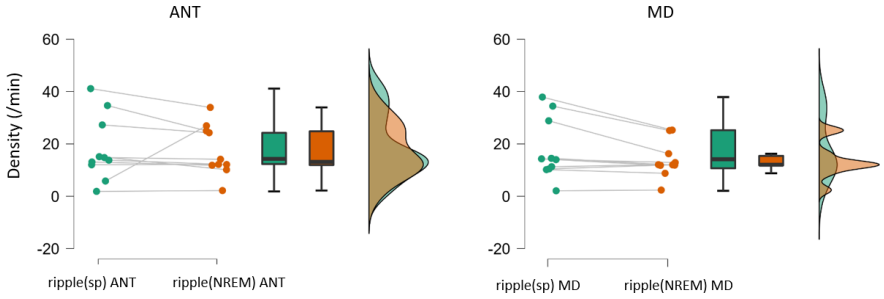

Figure 1. Ripple density in the ANT (left) and MD (right). Ripple(sp) reflects the ripple density during sleep spindles (ripple number / minute), ripple(NREM) reflects the density of ripples measured during the whole non-artifactual NREM sleep.

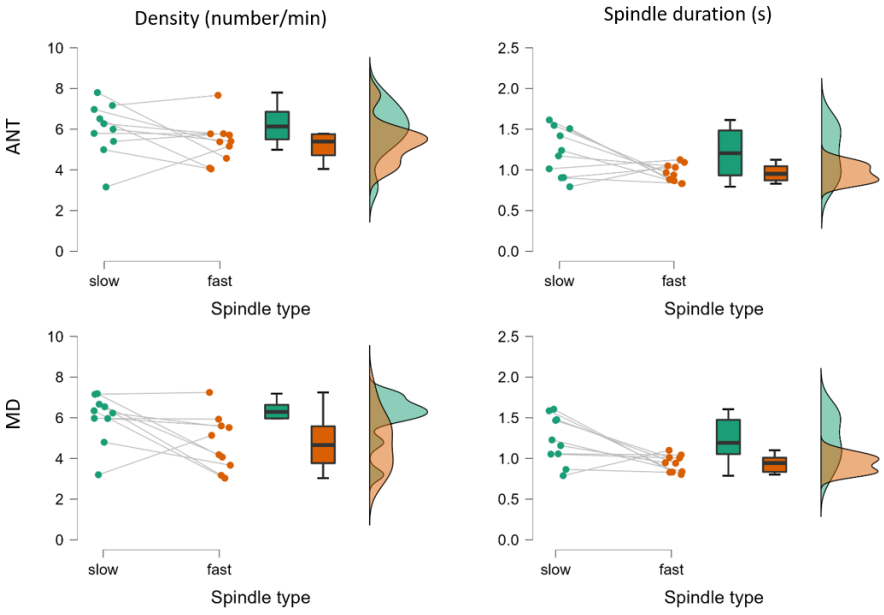

Figure 2. Overall sleep spindle density (left panel) and duration (right panel) in the ANT (top) and MD (bottom), separately for the slow spindles (green dots) and fast spindles (orange dots).

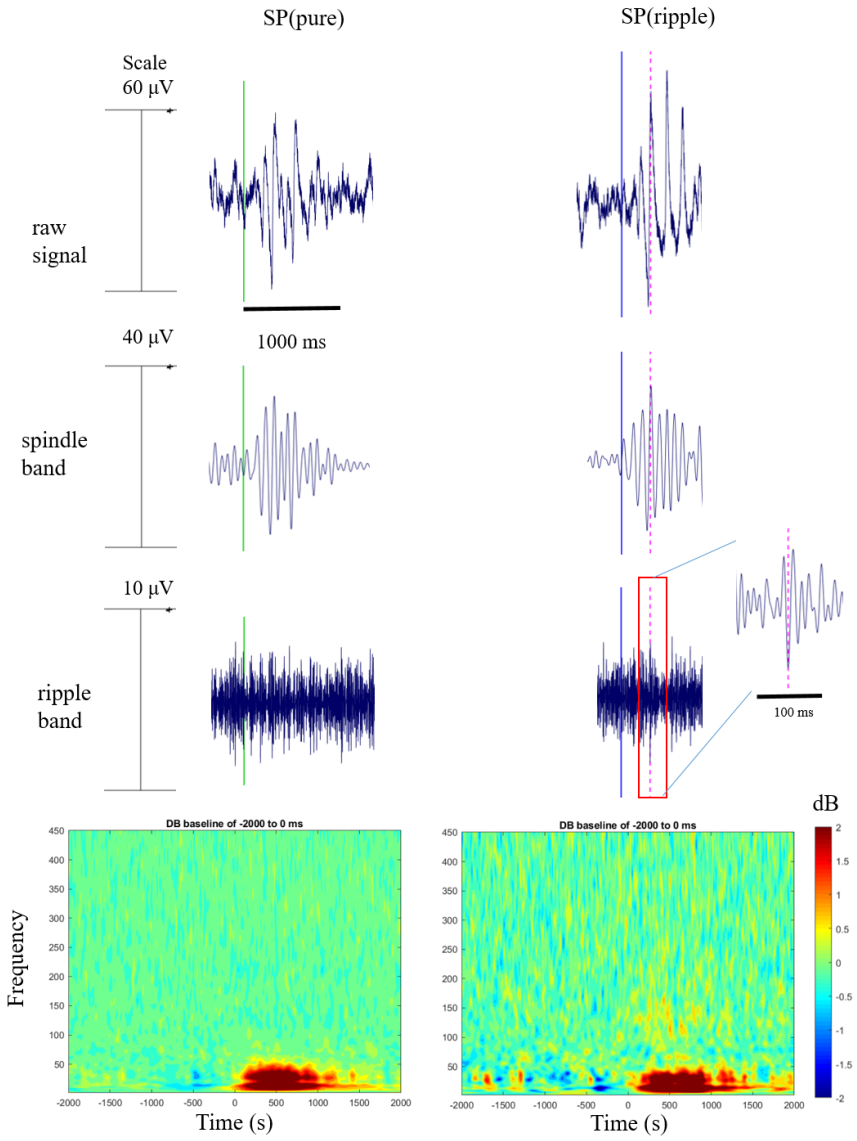

Figure 3. Examples of sleep spindles detected in the ANT from Patient #10: fast SP(pure) (left), and SP(ripple) (right). Upper row: 5 Hz highpass-filtered signal (raw signal), second row: 10–16 Hz bandpass-filtered signal (spindle band), third row: 100–200 Hz bandpass filtered signal (ripple band) of the same sleep spindle within each category. The fourth row depicts the time-frequency power spectra averaged across all fast sleep spindles of the same category detected in one ANT derivation of the same patient. The timepoint "0", and the green and blue lines indicate the onset of sleep spindles.

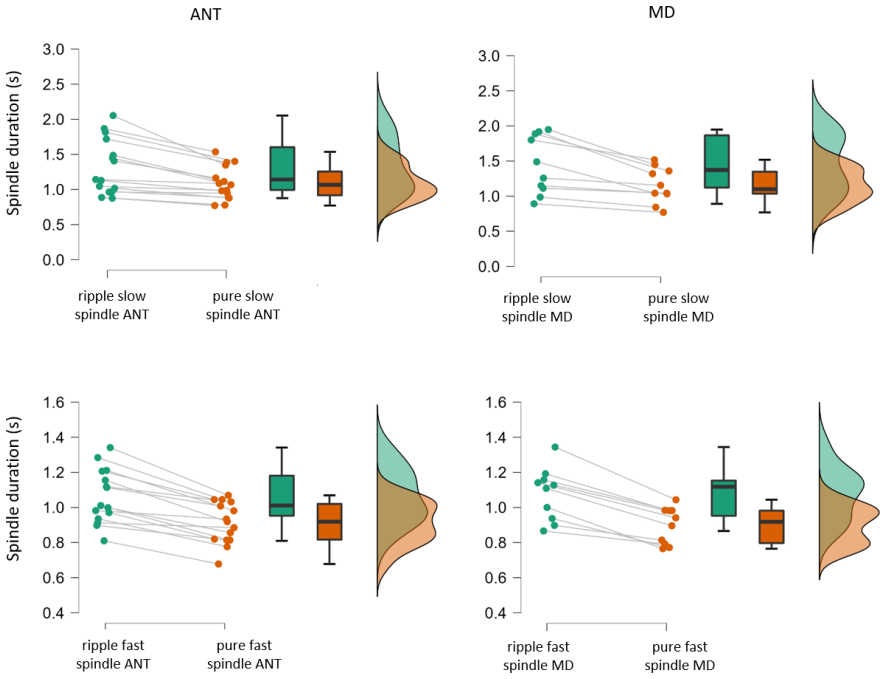

Figure 4. Sleep spindle duration in the ANT (left) and MD (right), separately for the ripple-associated and pure slow spindles (upper row) and fast spindles (bottom row). The green and orange dots represent the ripple-associated, and the pure sleep spindles, respectively.

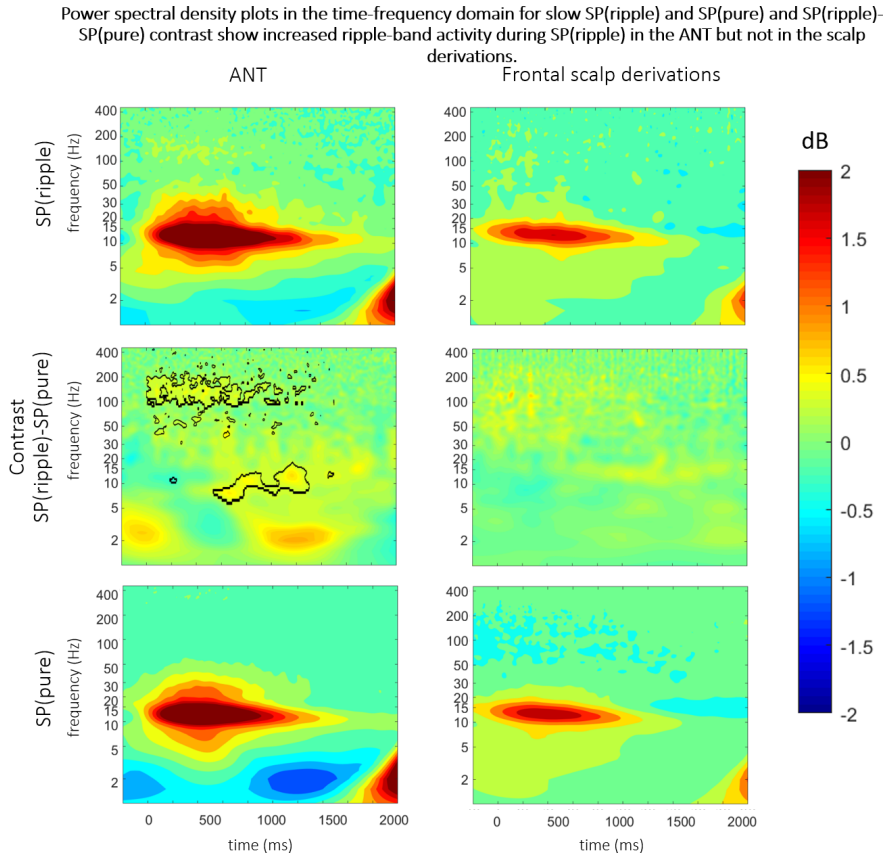

Figure 5. Power spectral density plots in the time-frequency domain for the slow sleep spindles measured in the ANT (left) and in the same time window in the frontal scalp derivations (right), separately for the SP(ripple) –top panels– and SP(pure) –bottom panels–, within the 1–450 Hz frequency range. The middle panels show the power spectral density differences between SP(ripple) and SP(pure). The timepoint "0" indicates the onset of sleep spindles in the ANT. Significant ($p< 0.05$ after FDR correction) time-frequency bins are circumscribed by the black lines. Increased time-frequency power was observed in the ripple and spindle band in the ANT but not in the scalp derivations. All time frequency maps were displayed from 2 to -2 dB, and frequency is represented in logarithmic scale.

Example for coupling between fast spindle phase and ripple amplitude in the ANT for patient #3

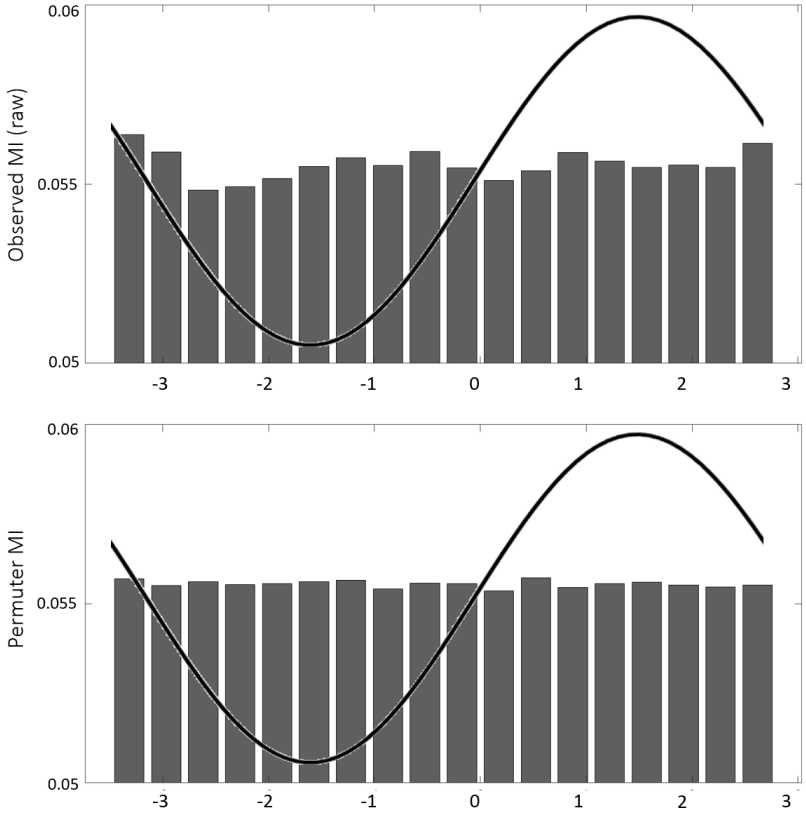

Figure 6. Example phase-amplitude coupling between fast spindle phase and ripple amplitude measured in the ANT for patient #3. MI(z) measured for this electrode position is 27.00, p<0.00001. The sine wave represents one cycle of the sleep spindle.

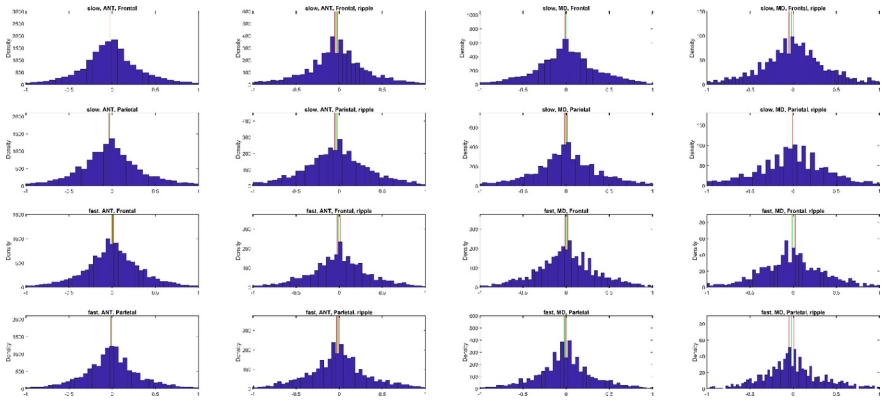

Figure 7. Thalamocortical spindle lags by ripple occurrence. Histograms show the time lag difference of scalp minus thalamic spindles by scalp region, thalamic nucleus, ripple presence and spindle type (slow or fast), pooled across all patients. Vertical green lines show the mean lag and red lines indicate the 95% CIs. Negative values indicate that spindles preferentially occur on the scalp first and vice versa. Axis X on each histogram is truncated at [-1 1] seconds

for optimal visibility.

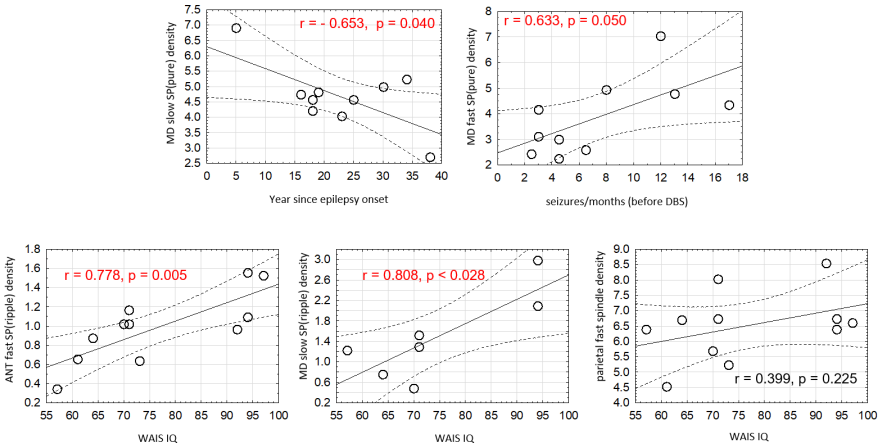

Figure 8. Correlations between clinical epilepsy characteristics, general intelligence and sleep spindle densities. The top left panel shows the significant negative correlation between epilepsy duration (year since epilepsy onset) and MD slow SP(pure) density. The top right panel shows the positive correlation between MD fast SP(pure) and seizure prevalence. The bottom left and middle panels show the significant positive correlations between general intelligence and SP(ripple) density in the ANT (left) and MD (middle). We did not find significant correlation with parietal scalp fast spindle density and IQ (right).

Table 1. Clinical and demographic data of the patients

Patient
#1
#2
#3
#4
#5
#6
#7
#8
#9
#10
#11
#12
#13
#14
#15

[1]bitemp – bitemporal; FO – foramen ovale electrodes; CR – controlled release; HS – hippocampal sclerosis; PVNH – periver

Table 2. Number of ANT and MD derivations for each patient

Patient	**Total number of ANT derivations**	**Left ANT derivations**	**Right ANT derivations**	**Total numbe**
#1	**1**	0	1	**1**
#2	**2**	0	2	**1**

Patient	Total number of ANT derivations	Left ANT derivations	Right ANT derivations	Total numbe
#3	**2**	0	2	**1**
#4	**3**	2	1	**0**
#5	**1**	1	0	**1**
#6	**4**	2	2	**0**
#7	**1**	0	1	**2**
#8	**6**	3	3	**0**
#9	**3**	1	2	**1**
#10	**3**	2	1	**2**
#11	**3**	2	1	**0**
#12	**2**	1	1	**2**
#13	**2**	1	1	**1**
#14	**4**	2	2	**0**
#15	**1**	0	1	**1**

Table 3. WAIS IQ scores for each patient

Patient	WAIS IQ
#1	**NaN**
#2	**NaN**
#3	**64**
#4	**61**
#5	**70**
#6	**97**
#7	**NaN**
#8	**92**
#9	**94**
#10	**71**
#11	**73**
#12	**71**
#13	**94**
#14	**NaN**
#15	**57**

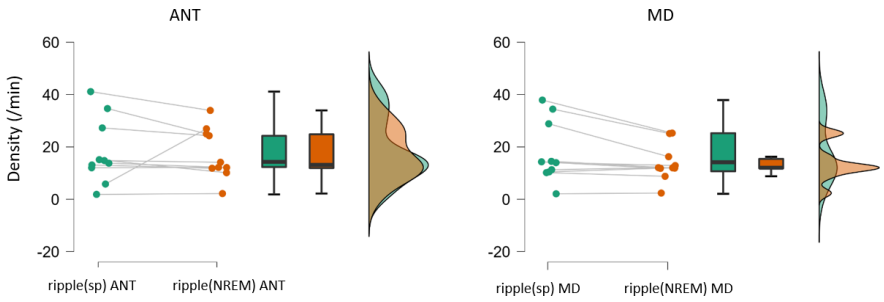

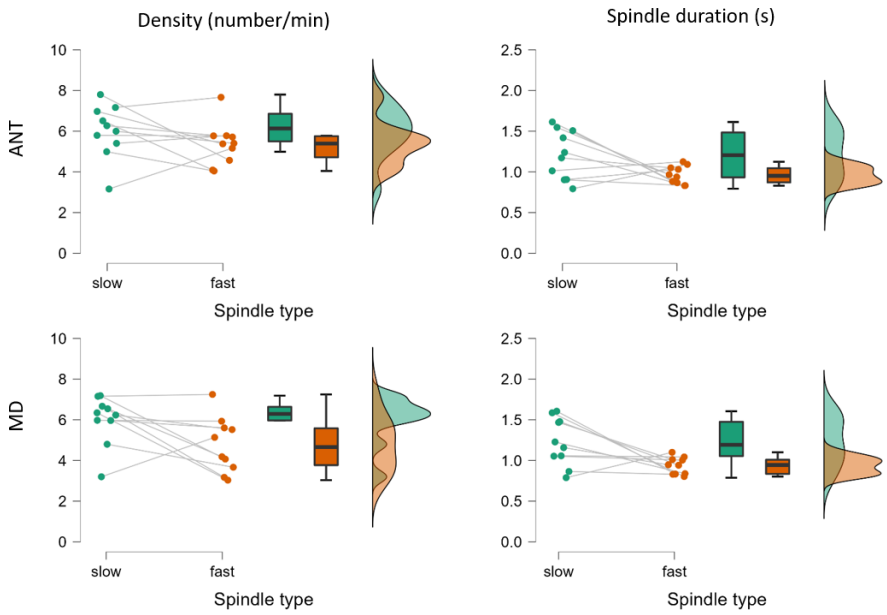

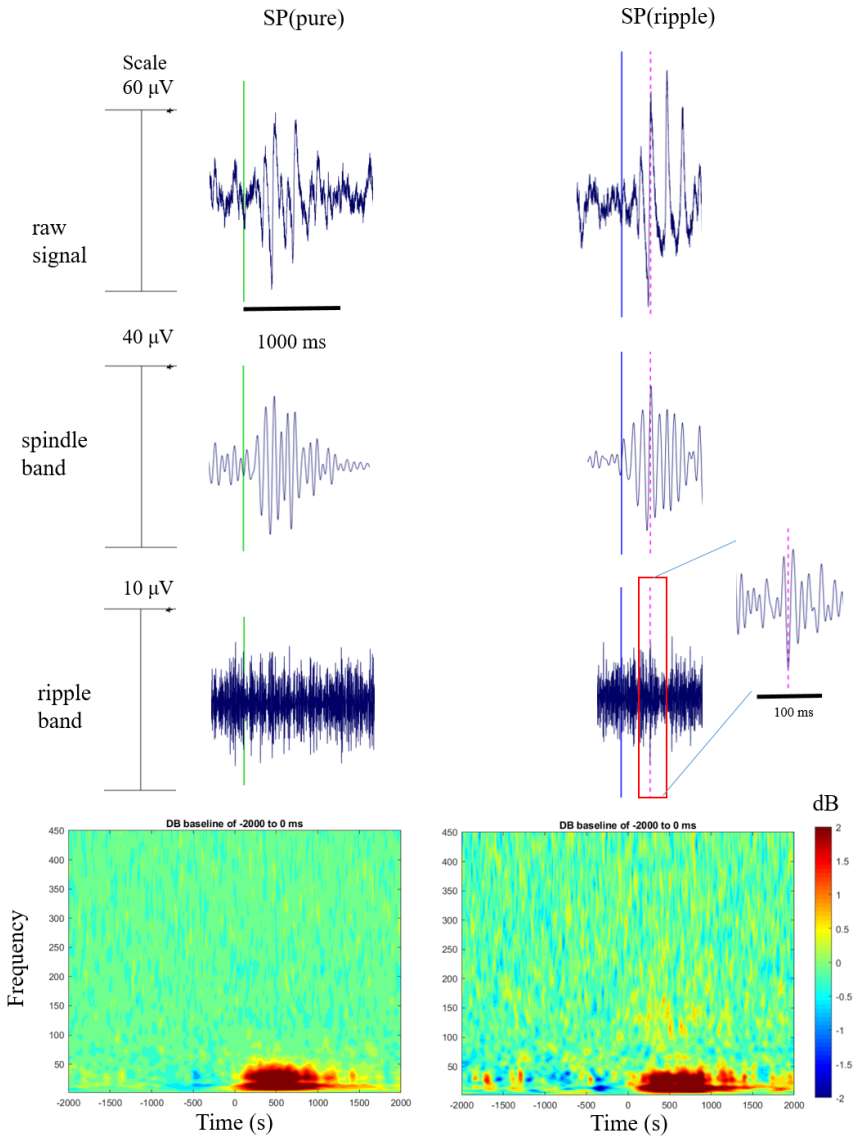

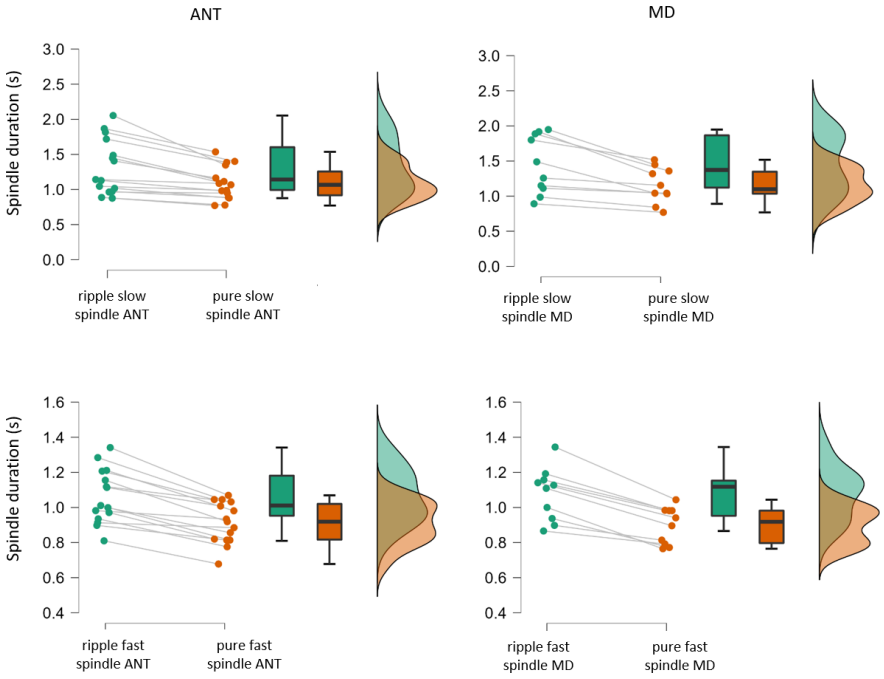

Power spectral density plots in the time-frequency domain for slow SP(ripple) and SP(pure) and SP(ripple)-SP(pure) contrast show increased ripple-band activity during SP(ripple) in the ANT but not in the scalp derivations.

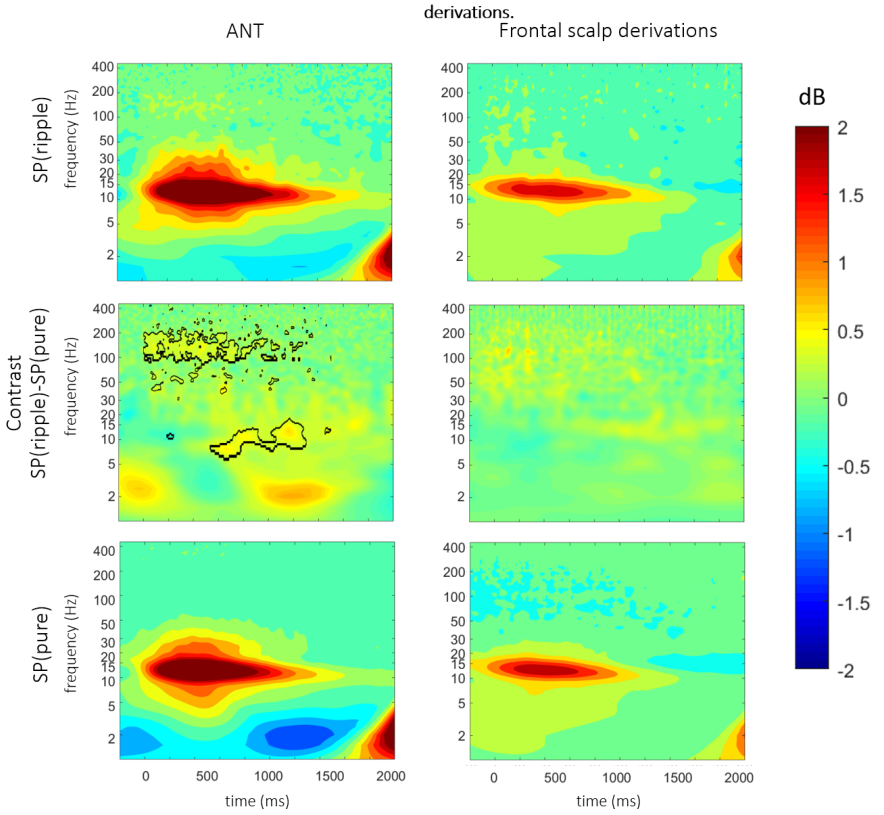

Example for coupling between fast spindle phase and ripple amplitude in the ANT for patient #3